The State Scientific Center of Russia
The Budker Institute of Nuclear Physics
SB RAS

V. Antsiferov

PARAMETERS OF THE DISCHARGE PLASMA OF SURFACE-PLASMA H^- ION SOURCES

Budker INP 97-46

НОВОСИБИРСК

Parametrs of the discharge plasma of surface-plasma H^- ion sources

V. Antsiferov

Budker Institute of Nuclear Physics SB RAS
630090 Novosibirsk, Russia

Abstract

The plasma of a high-current hydrogen-cesium glow discharge of planotron and Penning H^- ion sources was studied with the use of spectroscopic methods. The elemental and charge compositions of the plasma were determined. The temperature of hydrogen atoms was determined and the electron density was estimated. The density variation of hydrogen atoms, cesium atoms and molybdenum atoms (electrode material) and cesium ions during the discharge pulse with the space resolution along two coordinates was observed. Blocking up of cesium atoms and ions and molybdenum atoms near the cathode surface was found. The radiation energy of the discharge plasma was measured within the visible spectral range.

1. Introduction

Characteristics of the similar discharge plasma and the physical processes determining its parameters have not been studied completely, because the small plasma volumes, source magnetic field and cesium absorption hinder the use of the probe methods for non-disturbed measuring the parameters of the plasma. Spectroscopic methods are more faithful to study the parameters of the ion sources high-current discharge plasma. Such methods have a number of considerable advantages: the measurement contactless and the absence of perturbing action on the object; high sensitivity, high selectivity and high measurement rate; non-susceptibility to electromagnetic interference.

In this work we present the results of spectroscopic measurements of the H^- ion sources discharge plasma with planotron and Penning electrode geometries, published previously in[1–5].

2. Sources description

Electrodes of planotron (Fig. 1,a) and Penning(PIG) (Fig. 1,b) H^- ion sources were made of high-purity molybdenum. The external magnetic field **B** provided electrons oscillation in **E**×**B** crossed fields for planotron and in **E**||**B** — for the PIG. Purified hydrogen was fed into the discharge by the electromagnetic valve in the pulsed Mode, and cesium – from an external heated container with cesiated pyrographite in the continued Mode. The gas-discharge chamber of planotron and Penning sources had the following main parameters:

Discharge voltage, V	100 – 600
Discharge current, A	10 – 150
Pulse duration, μs	850 and 35
Pulse repetition rate, Hz	1 – 10
Magnetic field, kG	0.5 – 1.5
Cathode temperature, °C	400 – 800
Anode temperature, °C	200 – 400
Planotron cathode area, cm^2	5
The PIG cathode area, cm^2	2.5
Density of H_2, cm^{-3}	up to 10^{16}
Density of Cs, cm^{-3}	up to 10^{13}

Several stable Modes (I–IV) of the hydrogen-cesium discharge were observed, their voltages and volt-ampere characteristics being different (Fig. 1,e). The shapes of the current pulse (Fig. 1,d) and discharge voltages (Fig. 1,c) were close to rectangle. Mode IV was realized in pure-hydrogen discharge without cesium on the degassed by the pre-burn electrodes. Hydrogen-cesium Modes I–III differed in the amount of cesium deposited on the electrodes and were monitored by the electrode temperature and the cesium feed rate into the discharge.

Plasma radiation passed through the diagnostic slit of $0,2 \times 10$ mm^2 in the anode chamber, then through the collimation slit in the shutter inside the vacuum volume and through the quartz glass inside the wall of the vacuum chamber and was focused on the entrance slits of the detectors by the condenser. Anode chamber with four diagnostic slits I–IV (Fig. 1,b) was used in discharge spatial characteristics study. Plasma radiation in the near-cathode zone was studied through the slit I and here radiation radiated from the cathode surface and studied by the slit IV at plasma volume capture angle of 2° near cathode surface, did not pass through the slit (total angle acceptance of each slit was 12°). Plasma sections between the electrodes were observed through the slits II and III. Using of a number of the diagnostics slits and the shutter enabled us to determine components dynamics and the main plasma parameters of the PIG discharge with the spatial resolution along two coordinates. The spatial resolution along the coordinate while measuring the radiation of the discharge plasma was achieved by scanning the image of each diagnostic slit along the monochromator slit by moving the coudenser projecting the image of the diagnostic slit on monochromator slit. The image of diagnostic slit was parallel to the monochromator slit.

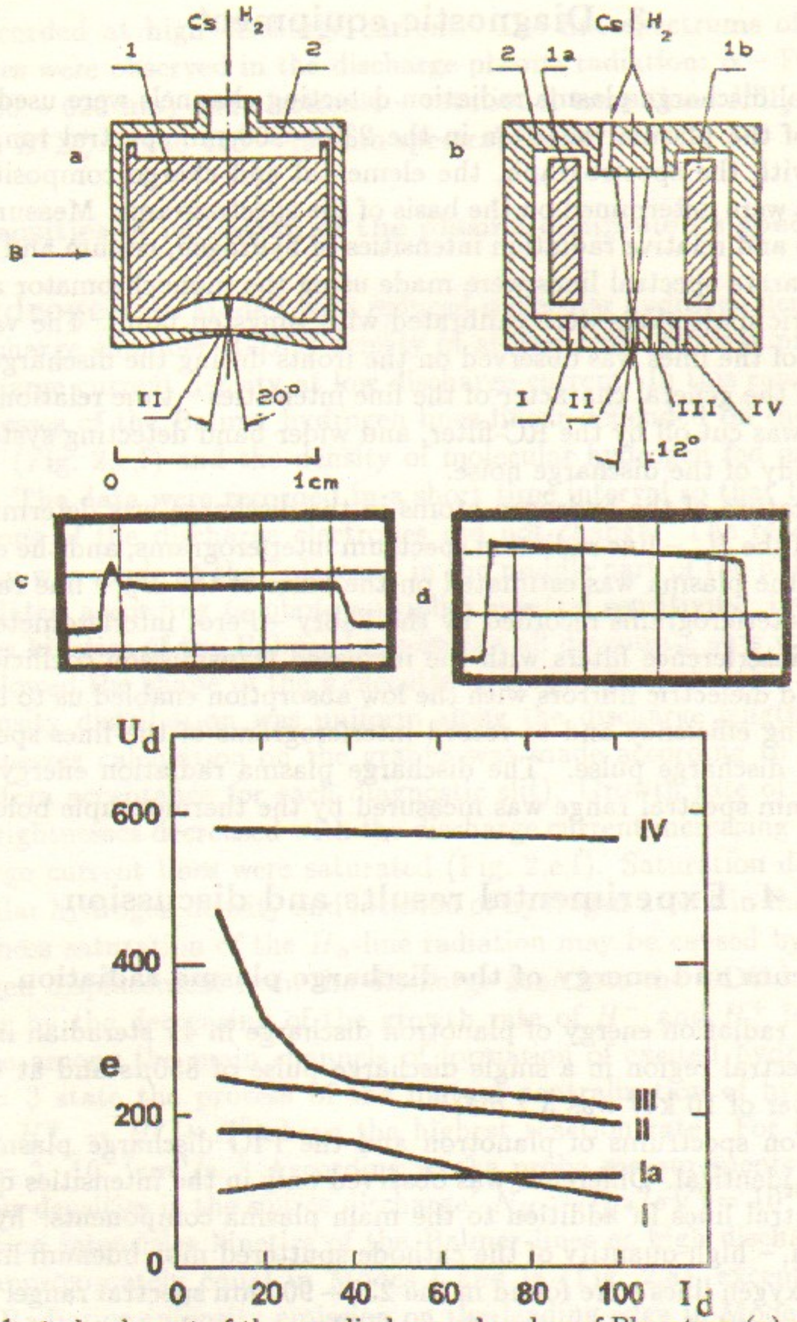

Figure 1: 1a,b – layout of the gas-discharge chamber of Planotron (a) and Penning (b) H^- ion sources: 1 – cathode, 2 – anode, B – magnetic field, I–IV – diagnostic slits; c, d – oscillograms of the current pulses (b) and of the source discharges voltage (c); scales: along the horizontal – 200 μs/division, along the vertical – 50 A (d) and 200 Volts (c); e – Volt-Ampere characteristics of the high-current glow H^- ion sources discharges.

3. Diagnostic equipment

Four optical discharge plasma radiation detecting channels were used. Spectrograms of the plasma radiation in the 230 – 900 nm spectral range were recorded with the spectrograph, the elemental and charge compositions of the plasma were determined on the basis of the spectrograms. Measurements of absolute and relative radiation intensities of hydrogen, cesium and molybdenum separate spectral lines were made using the monochromator and the photoelectric multipliers were calibrated with tungsten lamp. The variation intensities of the lines was observed on the fronts during the discharge pulse. In study of the general character of the line intensities – time relation, radiation noise was cut off by the RC-filter, and wider band detecting system was used in study of the discharge noise.

Temperature of the hydrogen atoms in the discharge was determined on the basis of the H_α – line radiation spectrum interferograms, and the electron density in the plasma was estimated on the basis of the H_β – line radiation spectrum interferograms recorded by the Fabry – Perot interferometers. Using of the interference filters with the increased transmission coefficient (up to 80%) and dielectric mirrors with the low absorption enabled us to increase the recording efficiency and to record interferograms of the lines spectrums in a single discharge pulse. The discharge plasma radiation energy in the 400 – 800 nm spectral range was measured by the thermocouple bolometer.

4. Experimental results and discussion

A. Spectrum and energy of the discharge plasma radiation

Plasma radiation energy of planotron discharge in 4π steradian in 400 – 800 nm spectral region in a single discharge pulse of $850\mu s$ and at the discharge power of 10 kW was 3.2 mJ.

Radiation spectrums of planotron and the PIG discharge plasma were practically identical. Difference was observed only in the intensities quantity of the spectral lines In addition to the main plasma components: hydrogen and cesium, – high quantity of the cathode sputtered molybdenum lines and impurity oxygen lines were found in the 230 – 900 nm spectral range. Identification was made for the spectral lines of Balmer series hydrogen atoms (H_α, H_β, H_γ, H_δ), for the lines of cesium atoms CsI, of singly – charged cesium ions CsII (300 – 650 nm), of doubly – charged cesium ions CsIII (250 – 290 nm), and for the lines of MoI atoms and of singly – charged molybdenum ions MoII. Transitions from the highly excited levels of cesium atoms ($n \sim 15$)

were recorded at high discharge current. The line spectrums of hydrogen molecules were observed in the discharge plasma radiation: α – Fulcher system (580 – 620 nm) and electronic – rotational transitions $I^1\Pi_g \rightarrow B^1\Sigma_g^+$, $G\Sigma_g^+ \rightarrow B^1\Sigma_u^+$ in the 420 – 490 nm spectral range.

B. Intensities of radiation of the plasma components spectral lines

Hydrogen. In Mode I with reduced molecular hydrogen density in the gas-discharge chamber (GDC) density of atomic hydrogen was proportional to discharge current density at low discharge current. In this case, radiation brightnesses of the Balmer hydrogen lines linear depended on the discharge current (Fig. 2,e,f) and the density of molecular hydrogen fed into the discharge. The data were recorded in a short time interval so that the thermal conditions of the discharge electrodes did not change. The reading of the intensity was made at the "plateau" in the middle part of the pulse and was recalculated according to photomultiplier spectral sensitivity. Radiation intensities kinetics of the Balmer lines on the all diagnostic slits was identical and followed the shape of the molecular hydrogen gas pulse (Fig. 2,b). Spatial density distribution was uniform along the discharge length (Fig. 2,d) (brightnesses calculation on the graphs was made according to the detecting system acceptance for each diagnostic slit). Growth rate of the Balmer lines brightnesses decreased with the discharge current increasing and at high discharge current lines were saturated (Fig. 2,e,f). Saturation depended on molecular hydrogen density and location of hydrogen atoms in the discharge. Brightness saturation of the H_α-line radiation may be caused by the partly hydrogen displacement from the discharge zone into the GDC lateral clearance or by the decreasing of the growth rate of H^- and H^+ ions density, because among the main channels of formation of excited hydrogen atoms in $n = 3$ state the process of the mutual neutralization of hydrogen ions ($H^- + H^+ \rightarrow H^* + H^0$) have the highest reaction rate. For this process $\langle\sigma V\rangle = 3 \cdot 10^{-7}\mathrm{cm}^3/\mathrm{s}$. [6] According to the probe measurements of H^- and H^+ ions densities in the source discharge[7] $N_{H^-} \cdot N_{H^+}\langle\sigma V\rangle = 10^{20}s^{-1} \cdot \mathrm{cm}^{-3}$. Radiation intensities kinetics of the Balmer lines at high discharge current were approximately equal in Modes I and Ia (Fig. 2,a), excepting leading edge. Radiation intensity emission on the leading edge in Mode I evidences of the relatively high atomic hydrogen contribution, desorbed from the GDC electrodes surface.

Values of the radiation intensities of the Balmer lines in Modes II–IV was approximately the same with those at appropriate discharge current in Mode

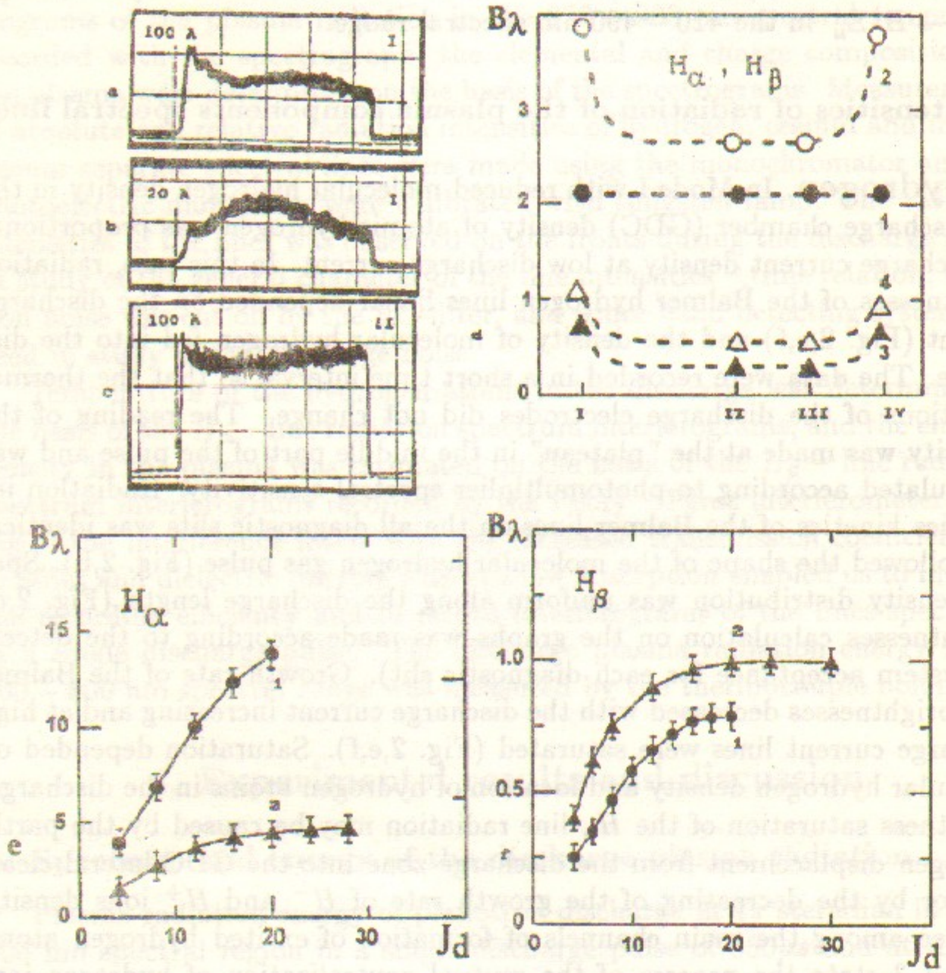

Figure 2: Parameters of the hydrogen Balmer lines radiation: a-c – oscillograms of the radiation intensities in Modes I (a,b) and II (c), scale: need vertical scales and units 200 μs/division; d – spatial distribution of the radiation brightnesses (B_λ) of the H_α – line (1,2) and of the H_β-line (3,4) over the diagnostic slits I–IV for the PIG in Mode I, the tables 1,2,3 and 4 in the plot of B_λ, vc.I,II,III and IV need explanation; e,f – radiation brightnesses (B_λ) of the H_α – line (e) and of the H_β – line (f) discharge current density relation for the Planotron (1) and for the PIG (2).

I, in spite of the increasing of the discharge voltage and higher hydrogen density in the GDC. Its kinetics followed the discharge current shape (Fig. 2,c). The rates of increasing and decreasing of the Balmer lines radiation intensities (leading and trailing edges of the radiation pulse) and the rates of increasing and decreasing of the discharge pulse current in this Modes were equal (to increase temporare resolution the shorter discharge pulse was used).

Cesium. Intensities and kinetics of the radiation of the cesium atoms lines and of the cesium ions lines substantially depended on the cesium feed into the discharge and on the thermal conditions of the electrodes.

Lines of the cesium atoms CsI (852.1 nm) with the highest force value of the transition oscillator ($f = 0.8$) have the maximum brightness in the $230 - 900$ nm spectral range. Figure 3,e shows the dependence of the CsI (852.1 nm) line radiation brightness on the discharge current density in Mode I for planotron and for the PIG (reading was taken on the basis of the intensity maximum at the end of the pulse). At a very low discharge current densities increasing of the electron and cesium densities in the discharge volume causes quadratic increase of the amplitude of the line radiation brightness. Then with the discharge current increase on a small value interval of its density, radiation brightness linear growth was observed. At high discharge current densities growth rate of the radiation brightness of the line abruptly dropped which is connected with the growth rate of cesium ionization and with its density decreasing in the interelectrode clearance.

At high discharge current the CsI (852.1 nm) line and the other cesium lines intensities increased at the end of the discharge pulse (Fig. 3,a,b). Long duration of the leading edges of the radiation pulse in Modes I and *Ia* depended on the additional cesium release into the discharge due to the electrode bombardment. Its sputtering coefficient is decreased in Mode I because of the increasing of the repeated ion – electron emission coefficient. Pulse overheating of surface by the discharge and the cesium release from the cooler, non-operating sections of the interelectrode clearance led to the equilibrium density increasing and to the cesium accumulation in the discharge. The CsI line intensity kinetics had the another character at low discharge currents and at high currents in Modes II and III (Fig. 3,c). Abrupt radiation intensity emission on the leading edge is caused by the cesium excitation in the discharge interval volume. Intensity increase at the end of the pulse is connected with the cesium release into the discharge due to the electrode bombardment. Rates of the increase of the cesium lines intensities increased at the beginning of the radiation pulses in Modes II and III in comparison with those in Mode I, but they were substantially lower then Balmer lines increase rates, here intensity decreasing at the end of the pulse proceeded

qsufficiently quicker. In Modes II and III with the hotter electrodes the initial cesium density in the GDC volume is higher then in Mode I, while the cesium concentration on the electrodes is low. In this case the sputtering coefficient of cesium is higher which causes cesium lines intensities fast reach a relatively high stationary level.

Spatial distribution of the CsI (852.1 nm) brightness over the diagnostic slits I-IV was substantially asymmetrical (Fig. 3,d), especially at high discharge currents. It evidences unambiguously that the emission cathode surface and plasma fitting thin layer which can be seen only through the slit IV give the determining contribution into the radiation of this line.

Symmetrical distribution of the CsI (455.5 nm) line brightness over the diagnostic slits (Fig. 4,c) shows that the radiation from the discharge volume gives the to make a contribution into the radiation of this lines. Besides, we observed a substantial difference in the intensity kinetics of this two lines in the discharge near the cathodes when the CsI (455.5 nm) line intensity saturation occurred at the beginning of the discharge pulse (Fig. 4,b). Here a character of dependence of the radiation intensity of this lines on time in the discharge center coincided (Fig. 4,a). CsI (455.5 nm) line radiation brightness saturation occurred at the lower discharge current densities (Fig. 4,d).

Cesium ions. Intensities kinetics of the cesium ion lines (Fig. 5,a) and intensities kinetics of the cesium atoms lines in Mode I were completely coincided. Increasing of the cesium electrons density and cesium ions density in the discharge in Mode II causes rapid quadratic increase of the amplitude of the radiation intensity of the cesium ions line at a discharge current increasing (Fig. 5c). Radiation brightnesses of the all cesium lines considerably increased in Mode Ia at forced cesium feed into the discharge when the discharge had become practically cesium – hydrogen. It led to little changes in intensities kinetics of the cesium lines (Fig. 5,b).

The spatial distribution of the brightnesses of the cesium ion lines and of the CsI (852.1 nm) line brightness over the diagnostic slits was abruptly asymmetrical, which evidences of the cesium ions blocking up near the cathodes. Here radiation brightnesses of the cesium ions lines near the cathodes in contrast to radiation brightness of the cesium atoms lines continued to increase at high current densities (up to $\sim$ 30 A/cm^2) (Fig. 5,e) and in the discharge center (on the slit II) they reached saturation at a current density of $\sim$ 10 A/cm^2. Comparison of radiation intensities of the cesium atoms lines and cesium ions lines shows that cesium was predominantly ionized during the discharge pulse in Modes I–III.

Molybdenum. The radiation brightnesses of the molybdenum atoms lines were minimal among the studied spectral lines. Molybdenum was

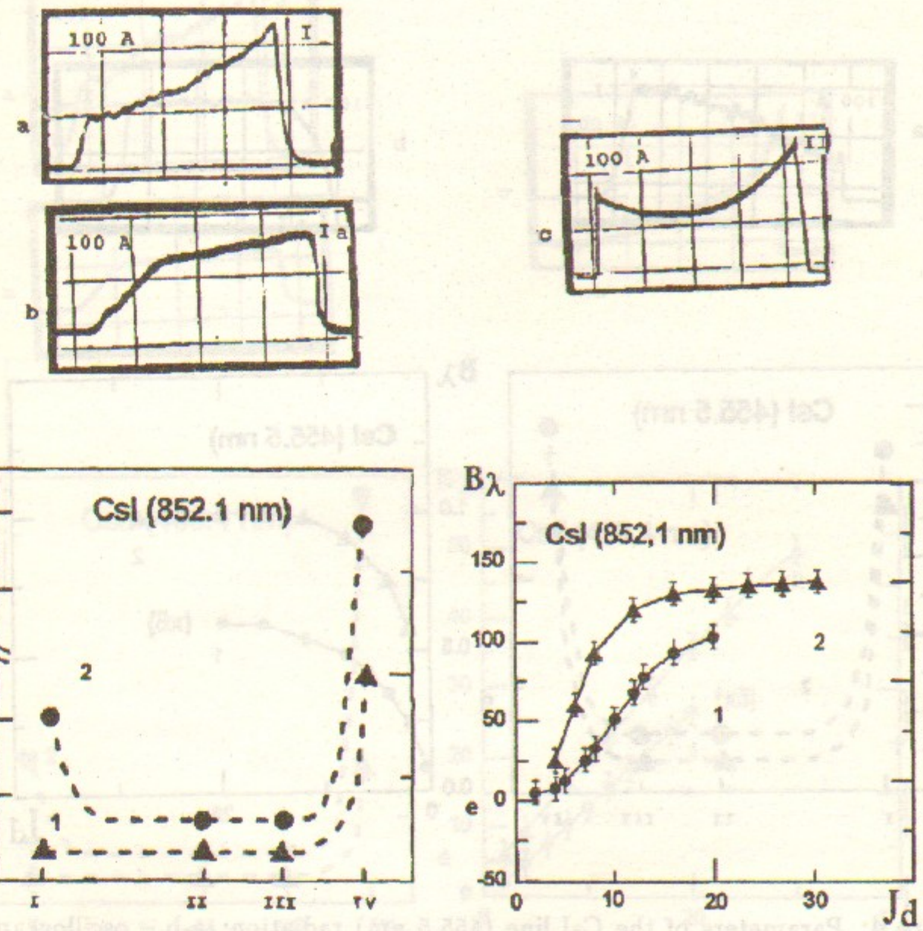

Figure 3: Parameters of the CsI line (852.1 nm) radiation: a-c – oscillograms of the intensities in I (a), Ia (b), II (c) Modes, need vertical scales and units 200 μs/division; d – spatial distribution of the lines brightnesses B_λ over the diagnostic slits I–IV in Mode I for the PIG; e – radiation brightnesses (B_λ) of the line discharge current density relations in Mode I for Planotron (1) and for the PIG (2).

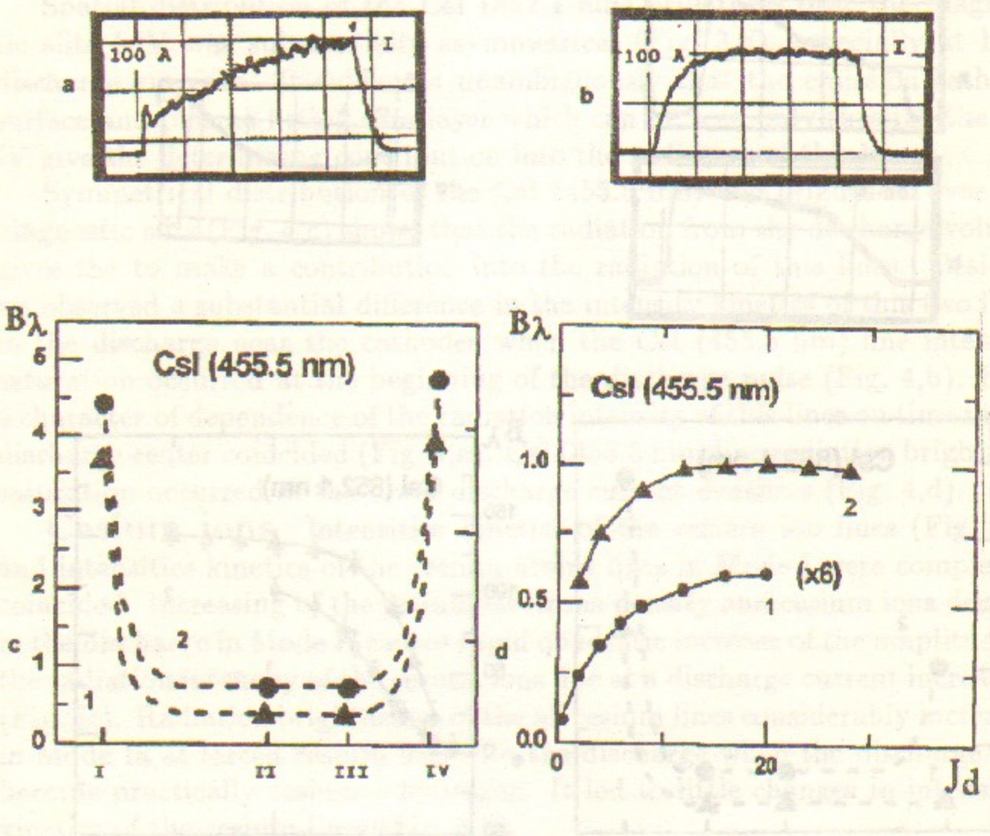

Figure 4: Parameters of the CsI line (455.5 nm) radiation: a-b – oscillograms of the intensities in Mode I, need vertical scales and units 200 μs/division; c – space distribution of the brightnesses B_λ over the diagnostic slits I–IV in Mode I for the PIG, the tables 1,2,3 and 4 in the plot of B_λ, vc.I,II,III and IV need explanation; d – radiation brightnesses (B_λ) of the line discharge current density relation in Mode I for Planotron (1) and for the PIG (2).

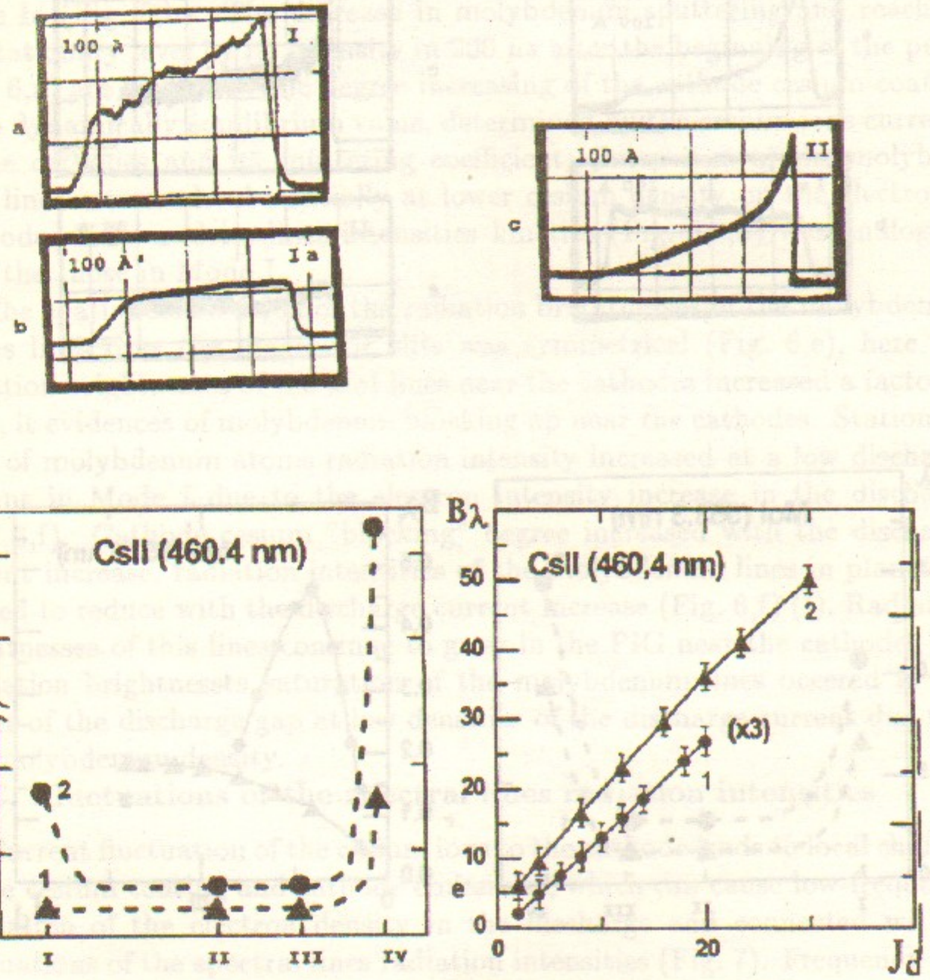

Figure 5: Parameters of the CsII line (460.4 nm) radiation: a-c – oscillograms of the intensities in Modes I (a), Ia (b) and II (c), need vertical scales and units 200 μs/division; d – spatial distribution of the line brightnesses B_λ over the diagnostic slits I–IV in Mode I for the PIG, the tables 1,2,3 and 4 in the plot of B_λ, vc.I,II,III and IV need explanation; e – radiation brightnesses (B_λ) of the line discharge current density relation in Mode I for Planotron (1) and for the PIG (2).

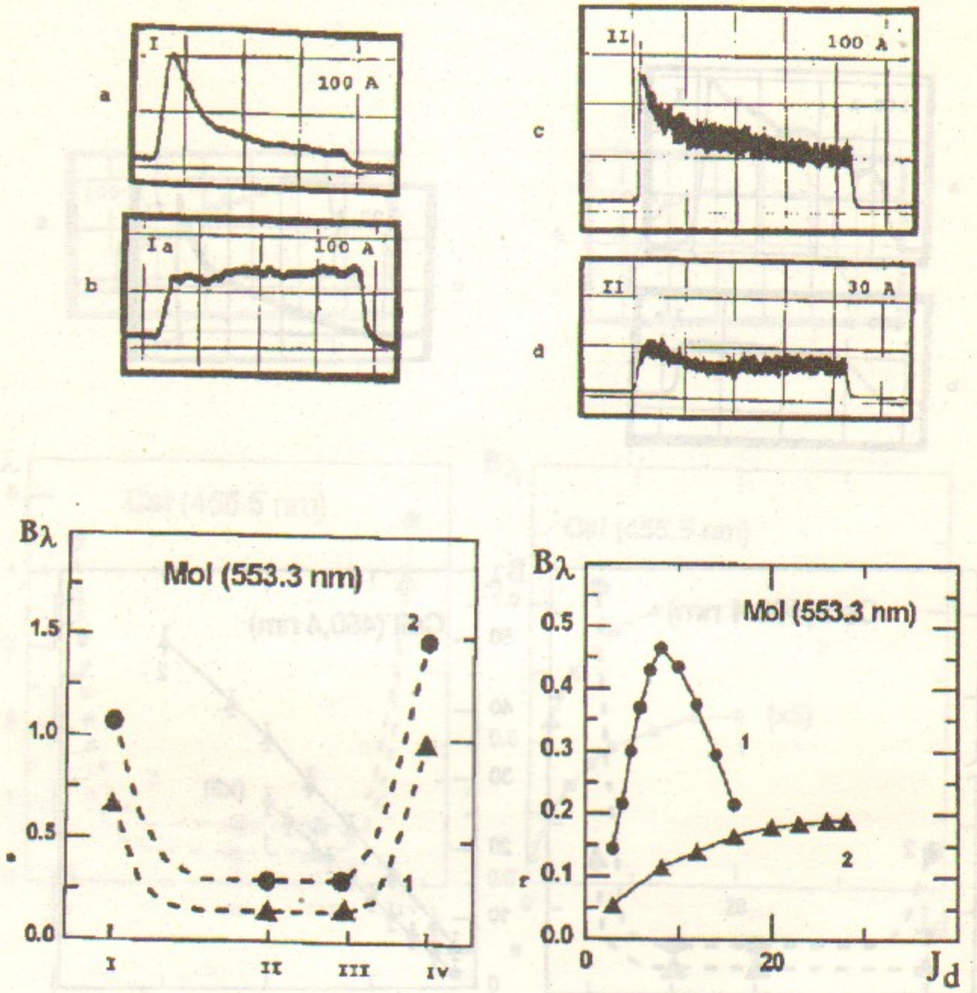

Figure 6: FIG. 6. Parameters of the MoI line (553.3 nm) radiation: a-d – oscillograms of the intensities in Modes I (a), Ia (b) and II (c,d), need vertical scales and units 200 μs/division; e – spatial distribution of the brightnesses (B_λ) over the diagnostic slits I–IV in Mode I for the PIG, the tables 1,2,3 and 4 in the plot of B_λ, vc.I,II,III and IV need explanation; f – radiation brightnesses (B_λ) of the line discharge current density relation in Mode I for Planotron (1) and for the PIG (2).

knocked-out of planotron and the PIG electrodes predominantly at the beginning of the gas-discharge pulse in ModeI (Fig. 6,a). Molybdenum emission and its excitation occurred more uniformly during the discharge pulse in more Mode Ia (Fig. 6,b). The decrease in molybdenum sputtering and reaching the stationary level by its intensity in 200 μs after the beginning of the pulse (Fig. 6,a) are caused by the degree increasing of the cathode cesium coating up to dynamically equilibrium value, determined by the cesium ions currents to the cathodes and its sputtering coefficient. Intensities of the molybdenum lines increased substantially at lower cesium density on the electrodes in Modes II-IV and its lines intensities kinetics (Fig. 6,c,d) was analogous with the those in Mode I.

The spatial distribution of the radiation brightnesses of the molybdenum atoms lines over the diagnostic slits was symmetrical (Fig. 6,e), here the radiation brightnesses of the MoI lines near the cathodes increased a factor of $2-3$, it evidences of molybdenum blocking up near the cathodes. Stationary level of molybdenum atoms radiation intensity increased at a low discharge current in Mode I due to the electron intensity increase in the discharge (Fig. 6,f). Cathode cesium "blocking" degree increased with the discharge current increase, radiation intensities of the molybdenum lines in planotron started to reduce with the discharge current increase (Fig. 6,f) (I). Radiation brightnesses of this lines continue to grow in the PIG near the cathodes (2). Radiation brightnesses saturation of the molybdenum lines occered in the center of the discharge gap at low densities of the discharge current due to a low molybdenum density.

C. Fluctuations of the spectral lines radiation intensities

Current fluctuation of the cesium ions to the cathode leads to local changes of the cesium coating and cathode emissivity, which can cause low-frequency oscillation of the electron density in the discharge and connected with it fluctuations of the spectral lines radiation intensities (Fig. 7). Frequency and level of low-frequency fluctuations ($\sim 10^6$ Hz) and noise (LFN) increased with the discharge current growth. However, relative level of the LFN, defined as the ratio of the root – mean – square value of fluctuations to the mean value of intensity, generally decreased with the discharge current growth. LFN level increased with the magnetic field increase and with the decrease of the hydrogen and cesium feed into the discharge (Fig. 7,e), here LFN level was substantially lower in Mode I (Fig. 7,c,d) than in Modes II and III (Fig. 7,a,b). Mode I was very sensitive to the cesium density in the discharge in the PIG, its insignificant decreasing led to different instabilities in the discharge and to in going from noise Mode to noiseless Mode during the dis-

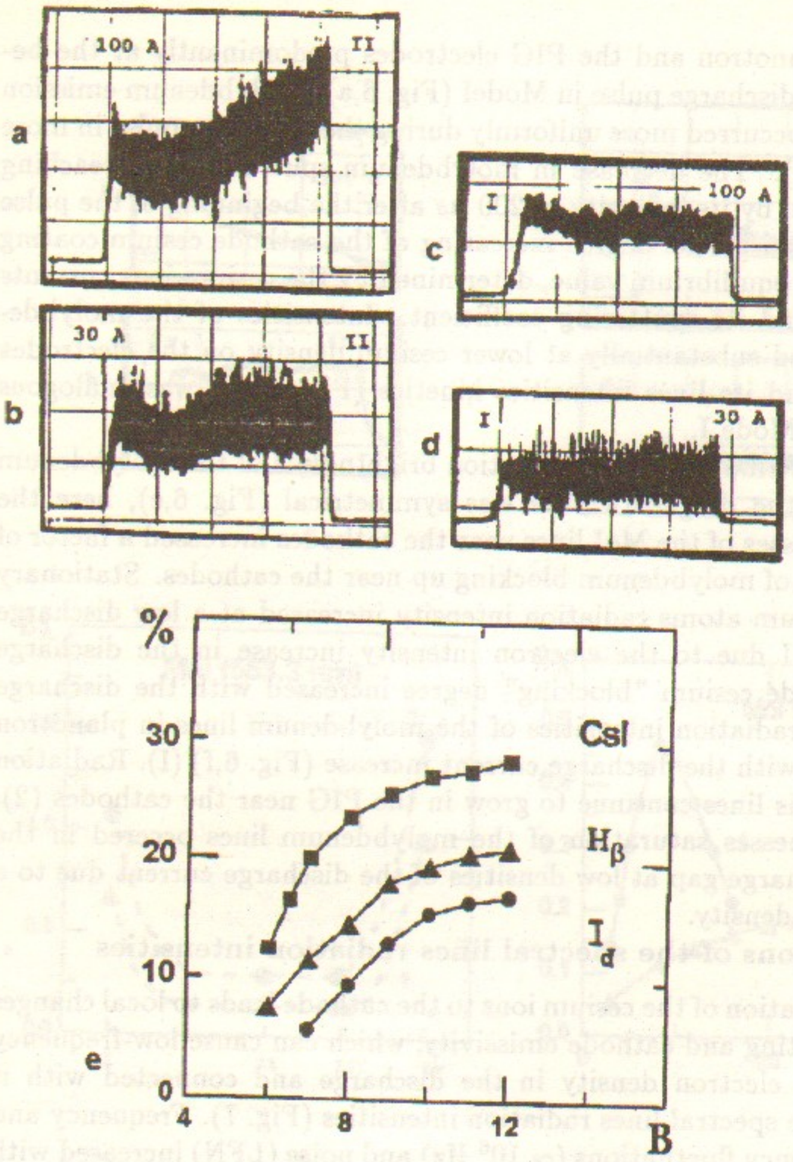

Figure 7: Parameters of the low-frequency fluctuations and noise (LFN) of the spectral lines radiation intensities and of the I_d discharge current: a-d – oscillograms of the CsI line (852.1 nm) radiation intensities in Mode I and of the H_β-line in Mode I, recorded by the bandwidth detecting system, need vertical scales and units 200 μs/division; e – dependence of the LFN relative level of the CsI and H_β – spectral lines and of the I_d discharge current on the value of the B external magnetic field.

charge pulse causing qualitatively modification of the intensity kinetics of the all spectral lines, excepting the molybdenum lines.

We observed a clear correlation between the intensities vibrations of the different spectral lines and vibrations of the current and of the voltage in the source discharge which unambiguously connected with the fluctuations of the H^- ions beam emittance extracted from the discharge by the field. Increase of the magnetic field from 0.6 to 0.9 kHz at a discharge current of 100 A led to increase of the current oscillations frequencies from 0.5 to 10 MHz and to H^- ions beam emittance value increasing practically a factor of 2. Increase of the beam emittance can be also connected with the growth of the magnetic field inhomogeneities of the source and with the increase of the space-charge potential beam.

D. Temperature of hydrogen atoms in the discharge

Temperature of hydrogen atoms in the discharge was determined by the doppler broadening of the H_α-line. Figure 8,a,b shows the typical interferograms of the H_α-line radiation spectrum for planotron and the PIG, recorded in a single discharge pulse. At microphotometering of the H_α-line spectrums interferograms fine structure of the H_α-line was not observed. It may be not taken into account if the predominant process of hydrogen atoms excitation is the dissociation of hydrogen molecules by the electron bombardment when 70% of the energy is radiated in the transition $3^2D_{5/2} \rightarrow 2^2P_{3/2}$. [8] In the pulsed discharge a considerable fraction of the hydrogen atoms was formed by desorption from the electrode surface which may lead to a broadening of the H_α-line contour. Broadening of the H_α-line contour is also due to the fine structure.

Temperature of hydrogen atoms in planotron and in the PIG linearly increased with the discharge current density growth (Fig. 8,c), here at low density of the discharge current ($\leq$ 20 A/cm^2) its values were considerably lower in planotron then in the PIG. Thus, for the production of the H^- accelerated beams with the minimum possible divergence planotron as a source is more preferable.

E. Density and temperature of electrons in the discharge plasma

Density of electrons in the discharge plasma was estimated by the Stark broadening of the H_β-line. Figure 8,d shows one of the H_β-line spectrum interferograms. Electrons density linearly depended on the discharge current

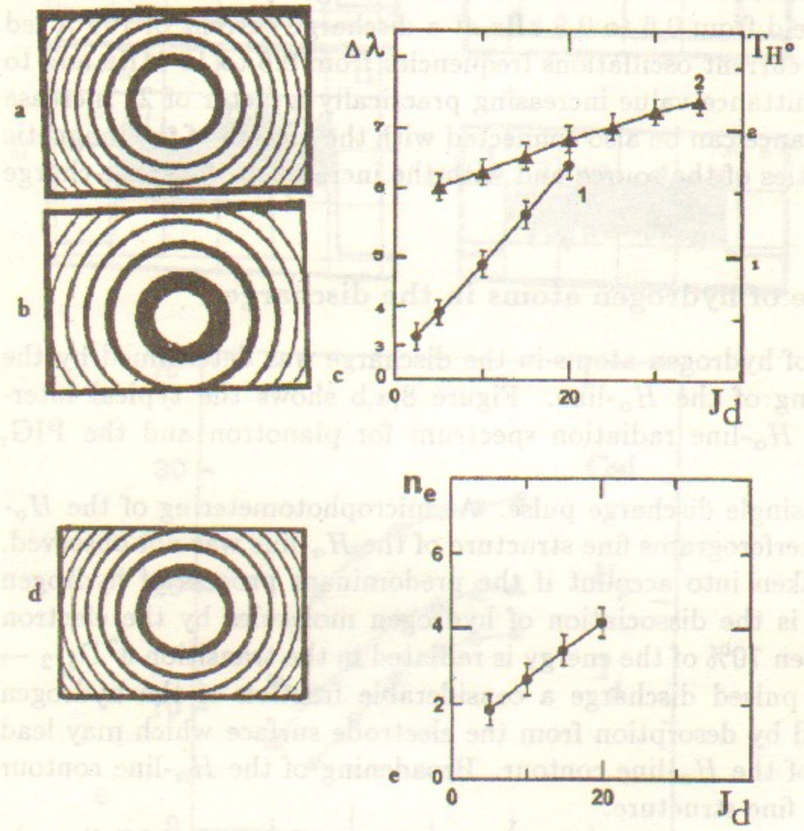

Figure 8: a,b – interferogram of the radiation spectrums of the H_α-line in Planotron (a) and in the PIG (b); c – dependence of the kT_{H^0} hydrogen atoms temperature and of H_α-line contour width on discharge current density in Mode I in Planotron (1) and in the PIG (2); d – interferogram of the radiation spectrum of the H_β-line in Mode I in Planotron; e – dependence of the electron density (n_e) in Planotron discharge in Mode I on the discharge current density (I).

density, at current density of 20 a/cm^2 its value was $4 \cdot 10^{13}$cm^{-3} (Fig. 8,e).

Temperature of electrons in the discharge was found from the relation between the Balmer lines intensities in local termodynamical equilibrium (LTE) approximation and Maxwell energy distribution of electrons. It was calculated according to the procedure of[9] and its value was 0.4 eV. Anomalously low electrons temperatures were obtained when we compared the intensities of different cesium lines and also from the distribution of intensities in the recombination continuum spectrum at the $5d$ level (550 – 590 nm). [10]. The "cesium" temperature of electrons was $\sim 0,1$ eV and it depended slightly on the cesium density.

The extremely low values of the electron temperature evidence that the use of the LTE model is limited in the conditions of high current glow discharge with the non-equilibrium character of the processes on the electrode surface. In this case, together with the low energy cluster of Maxwell electrons it is necessary to take into account the role of the cluster of the fast primary electrons.

5. Discussion

The use of the spectroscopic methods allowed us to realize non-perturbed control and to measure reliable the main parameters of the discharge plasma of surface – plasma H^- ion sources. It gives the possibility to construct a real theoretical model of this sources. Planotrons which have the lower temperature of hydrogen atoms in the discharge plasma at the equal discharge current densities than Penning sources were showed to be preferably used as sources for the production of the H^- ion accelerated beams with the minimum possible divergence.

References

[1] *V.V. Antsiferov, V.V. Beskorovaynyy, Yu.I. Belchenko, et al.//* Preprint Budker INP. N 88-116. Novosobirsk. 1988. 21 p.

[2] *V.V. Antsiferov, V.V. Beskorovaynyy, Yu.I. Belchenko, et al.//* AIP Conf. Proc. 1990. N 210. P.427-447.

[3] *V.V. Antsiferov, V.V. Beskorovaynyy.//* J.Techn. Physics. 1993. V.63. N 4. P.50-57.

[4] *V.V. Antsiferov, V.V. Beskorovaynyy.//* J.Techn. Physics. 1993. V.63. N 5. P.41-47.

[5] *V.V. Antsiferov.* //Preprint Budker INP. N 93-49. Novosibirsk. 1993. 23 p.

[6] *R.K. Janev.//* Report PPPL-TM-368. 1985. 20 p. q

[7] *Yu.I. Belchenko, G.I. Dimov, V.G. Dudnikov, A.S. Kupriyanov.//* Preprint Budker INP. N 88-14. Novosibirsk. 1988. 36 p.

[8] *G.N. Polyakova, A.I. Ranyuk, V.F. Yerko.//* J.Exper. Teor. Phys. 1977. V.73. N 6. P.2131-2141.

[9] *H.V. Smith, P. Allison.* //AIP Conf. Proc. 1987. N 158. P.181-192.

[10] *B.Ya. Moizhes, G.E. Pikus.//* Thermoemissive Converters and Low-Temperature Plasma. Moscow.: Nauka. 1973. 480 p.

V.V. Antsiferov

Parameters of the discharge plasma
of surface-plasma H^- ion sources

Budker INP 97-46

В.В. Анциферов

Параметры плазмы разряда поверхностно-плазменных
источников ионов H^-

ИЯФ 97-46

Ответственный за выпуск А.М. Кудрявцев
Работа поступила 28.04.1997 г.

Сдано в набор 21.04.1997 г.
Подписано в печать 7.05.1997 г.
Формат бумаги 60×90 1/16 Объем 1.5 печ.л., 1.2 уч.-изд.л.
Тираж 150 экз. Бесплатно. Заказ N 46.

Обработано на IBM PC и отпечатано на
ротапринте ГНЦ РФ "ИЯФ им. Г.И. Будкера СО РАН",
Новосибирск, 630090, пр. академика Лаврентьева, 11.